The Unusal Redox Centers of SoxXA, a Novel *c*-Type Heme-Enzyme Essential for Chemotrophic Sulfur-Oxidation of *Paracoccus pantotrophus*†

Edward J. Reijerse,*,‡ Monika Sommerhalter,‡,§ Petra Hellwig,|| Armin Quentmeier,⊥ Dagmar Rother,⊥ Christoph Laurich,‡ Eberhard Bothe,‡ Wolfgang Lubitz,‡ and Cornelius G. Friedrich*,⊥

Max-Planck-Institut für Bioanorganische Chemie, Stiftstrasse 34-36, D-45470 Mülheim/Ruhr, Germany, Institut Chimie UMR7177, Laboratoire de spectroscopie vibrationnele et électrochemie des biomolécules, Université Louis Pasteur, 4, rue Blaise Pascal, 67070 Strasbourg, France, and Lehrstuhl für Technische Mikrobiologie, Fachbereich Bio- und Chemieingenieurwesen, Universität Dortmund, Emil-Figge-Strasse 66, D-44221 Dortmund, Germany

Received February 20, 2007; Revised Manuscript Received April 24, 2007

ABSTRACT: The heterodimeric hemoprotein SoxXA, essential for lithotrophic sulfur oxidation of the aerobic bacterium *Paracoccus pantotrophus*, was examined by a combination of spectroelectrochemistry and EPR spectroscopy. The EPR spectra for SoxXA showed contributions from three paramagnetic heme iron centers. One highly anisotropic low-spin (HALS) species ($g_{max} = 3.45$) and two "standard" cytochrome-like low-spin heme species with closely spaced *g*-tensor values were identified, LS1 ($g_z = 2.54$, $g_y = 2.30$, and $g_x = 1.87$) and LS2 ($g_z = 2.43$, $g_y = 2.26$, and $g_x = 1.90$). The crystal structure of SoxXA from *P. pantotrophus* confirmed the presence of three heme groups, one of which (heme 3) has a His/Met axial coordination and is located on the SoxX subunit [Dambe et al. (2005) *J. Struct. Biol. 152*, 229−234]. This heme was assigned to the HALS species in the EPR spectra of the isolated SoxX subunit. The LS1 and LS2 species were associated with heme 1 and heme 2 located on the SoxA subunit, both of which have EPR parameters characteristic for an axial His/thiolate coordination. Using thin-layer spectroelectrochemistry the midpoint potentials of heme 3 and heme 2 were determined: $E_{m3} = +189 \pm 15$ mV and $E_{m2} = -432 \pm 15$ mV (vs NHE, pH 7.0). Heme 1 was not reducible even with 20 mM titanium(III) citrate. The E_{m2} midpoint potential turned out to be pH dependent. It is proposed that heme 2 participates in the catalysis and that the cysteine persulfide ligation leads to the unusually low redox potential (−436 mV). The pH dependence of its redox potential may be due to (de)protonation of the Arg247 residue located in the active site.

The oxidation of reduced inorganic sulfur compounds to sulfuric acid represents one-half of the global sulfur cycle. This oxidative part is mediated by various aerobic lithotrophic and anaerobic phototrophic sulfur-oxidizing bacteria (*1*−*3*). The sulfur-oxidizing (Sox) enzyme system of the facultatively chemolithoautotrophic α-proteobacterium *Paracoccus pantotrophus* (*4*) has been characterized with respect to the Sox proteins reconstituting the enzyme system in vitro. The *sox* genes encode the respective proteins and those required in addition to enable chemotrophic growth.

The Sox enzyme system of *P. pantotrophus* is located in the periplasm. Four proteins, SoxYZ, SoxB, SoxCD, and SoxXA, catalyze the hydrogen sulfide-, sulfur-, thiosulfate-, and sulfite-dependent reduction of horse heart cytochrome *c* in vitro (*4*−*6*). The proposed cycle of sulfur oxidation by the Sox enzyme system is depicted in Figure 1. The

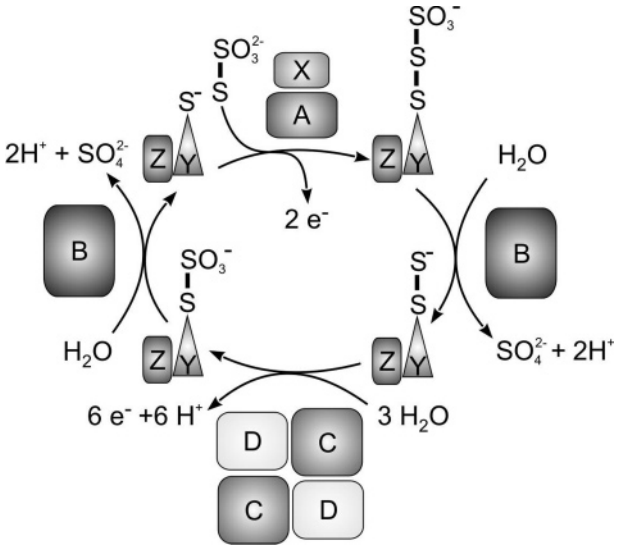

FIGURE 1: Model of protein-bound oxidation of thiosulfate to sulfate in *P. pantotrophus.* The capital letters indicate the Sox proteins according to their gene designation. X, A, cytochrome complex SoxXA; B, dimanganese protein SoxB; CD, heterotetrameric molybdoprotein−cytochrome *c* complex $Sox(CD)_2$ (adapted from ref *2*).

sulfhydryl of the single conserved Cys138 residue at the carboxy terminus of the SoxY subunit (10977 Da) of the

† This work was supported by the Max Planck Society and by Grants Fr 318/8-1 and Fr 318/6-1 of the Deutsche Forschungsgemeinschaft.

* Corresponding authors. E.J.R.: phone, +49-208-306-3529; fax, +49-208-306-3955; e-mail, reijerse@mpi-muelheim.mpg.de. C.G.F.: phone, +49-(0)231 755 5115; fax, +49-(0)231 755 5118; e-mail, cornelius.friedrich@udo.edu.

‡ Max-Planck-Institut für Bioanorganische Chemie.

§ Present address: Department of Chemistry and Biochemistry, California State University, East Bay, Hayward, CA 94542.

|| Université Louis Pasteur.

⊥ Universität Dortmund.

10.1021/bi7003526 CCC: $37.00
Published on Web 06/05/2007

heterodimeric SoxYZ protein is the active site of protein-bound oxidation of sulfur (*7*). The sulfur dehydrogenase SoxCD is a $\alpha_2\beta_2$ heterotetrameric complex of the molybdoprotein SoxC (43442 Da) and the diheme *c*-type cytochrome SoxD (37637 Da) (*8*). This complex oxidizes the protein-bound sulfur to sulfate (*3*, *6*, *9*). The monomeric dimanganese SoxB protein (58611 Da), which recently has been characterized using advanced EPR[1] methods (*10*), is proposed to hydrolyze sulfate from SoxY-cysteine *S*-sulfate to regenerate SoxY (*3*). The heterodimeric SoxXA is a *c*-type cytochrome complex composed of the monoheme SoxX (14216 Da) and the diheme SoxA (29352 Da). The SoxXA complex is proposed to fuse the sulfur substrate to the sulfhydryl Cys138 of SoxY to initiate the reaction cycle (*4*).

Homologues of the Sox proteins of *P. pantotrophus* such as SoxX, -Y, -Z, -A, and -B have been identified from the genomes and partial genomic sequences of other aerobic chemotrophic and anaerobic phototrophic sulfur-oxidizing bacteria, suggesting a similar principal mechanism of sulfur oxidation in chemotrophic and phototrophic bacteria (*3*). In vitro studies revealed the essentiality of the *c*-type cytochrome complex SoxXA for the sulfur-oxidizing enzyme system of *P. pantotrophus* (*4*, *6*). Also, insertional mutagenesis in the *soxXA* genes demonstrated the presence of the *sox* genes to be essential for sulfur oxidation in the aerobic chemotrophic α-proteobacterium *Protaminobacter salicylatoxidans* (*11*) and the anaerobic phototrophic purple nonsulfur bacterium *Rhodovulum sulfidophilum* (*12*).

According to the designation of Cheesman et al. (*13*) and Dambe et al. (*14*) heme 1 is located in the N-terminal domain of SoxA and heme 2 is in its carboxy-terminal domain, while heme 3 is located in the small subunit SoxX. Multiple sequence alignments of the primary structures predicted an invariant methionine residue as the axial heme iron ligand for heme 3 of SoxX (*12*), which was in accordance with spectroscopic studies (*13*). For the SoxA subunit cysteine residues were predicted as the sixth ligand of heme 1 and heme 2 (*12*). These assignments have been confirmed in the X-ray structures of SoxXA in *R. sulfidophilum* (*15*) and *P. pantotrophus* (*14*). Figure 2 shows the coordination structure of the hemes in SoxXA of *P. pantotrophus* as defined by its crystal structure (*14*). Heme 1 has a classical His/Cys axial coordination (His110 and Cys143) while heme 2 turns out to have its cysteine modified into a cysteine persulfide ligand (His210 and Css251). This may have a strong effect on its redox potential (vide infra). Heme 3 in subunit X has a His/Met coordination (His65 and Met111). In SoxA of the SoxAX complex of the sulfur-oxidizing chemotroph, *Starkea novella*, however, heme 1 is replaced by a disulfide (*16*). According to the crystal structures of the SoxXA complex of *R. sulfidophilum* (*15*) and *P. pantotrophus* (*14*) the subunits form a cleft suited to fit in the carboxy-terminal end of SoxY which reaches toward heme 2 which is believed to be the active site of the enzyme. However, the actual mechanism of how the sulfur substrate is fused to the sulfhydryl of SoxY is not yet understood.

Here, we describe the electrochemical and EPR spectroscopic properties of the *c*-type cytochrome complex SoxXA of *P. pantotrophus*. We have isolated the SoxX subunit,

[1] Abbreviation: EPR, electron paramagnetic resonance.

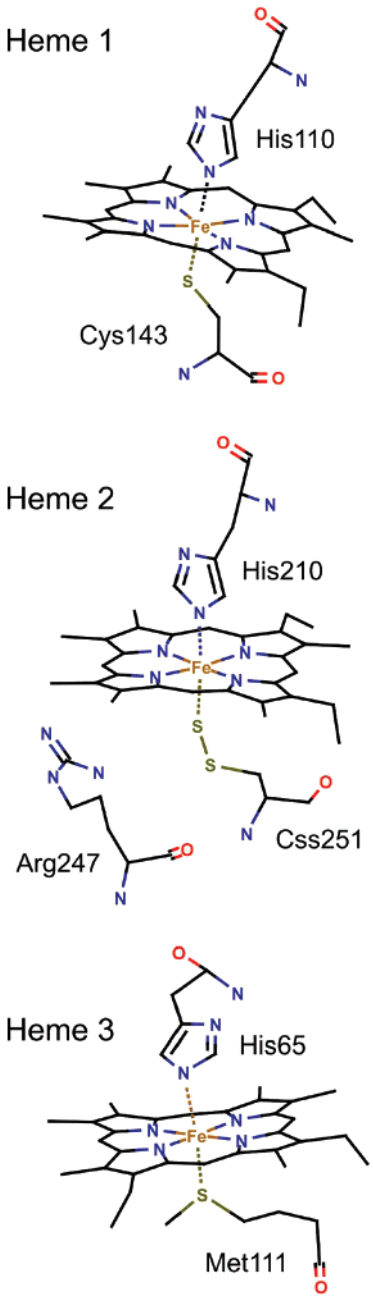

FIGURE 2: Coordination structures of the heme cofactors in the SoxXA protein according to the X-ray data (*14*) (PDB file 1C2D. Heme 1 and heme 2 are present in chain A (SoxA subunit) while heme 3 is bound to chain B (SoxX subunit).

identified the axial heme ligands of its heme 3, and determined the heme 3 redox potential. Heme 2 of SoxA was found to be also redox active. Heme 1, however, could not be reduced.

MATERIALS AND METHODS

Purification of SoxXA and SoxX. The heterodimeric cytochrome complex SoxXA was purified to homogeneity from *P. pantotrophus* GB17 cultivated lithoautotrophically with thiosulfate as described previously (*6*). The SoxX subunit of SoxXA of *P. pantotrophus* was produced in *Escherichia coli* and prepared from periplasmic extracts as described (*17*). SoxX was isolated from 200 mL of periplasmic extract and concentrated to 8 mL. Proteins were separated by chromatography on Q-Sepharose, and SoxX was

eluted from a step gradient at 0.15 M sodium chloride in a 25 mM potassium phosphate buffer, pH 7.5. The concentration of the eluate resulted in 0.75 mL of a homogeneous preparation of 1.32 mg of SoxX/mL, equivalent to 94 μM SoxX.

Electrochemistry. Electrochemical reduction of the SoxXA protein complex monitoring the optical absorbance changes in situ was performed in two different spectroelectrochemical thin-layer cells.

The ultrathin layer cell for the UV/vis detection was used as previously described (*18*, *19*). The gold grid working electrode was chemically modified with a 1:1 mixture of 2 mM cysteamine and 2 mM mercaptopropionic acid in aqueous solution. Potentials quoted with the data have been obtained vs a Ag/AgCl/3 M KCl reference electrode: for NHE potentials (pH 7) a correction of +208 mV has been added. All measurements were performed at 5 °C, and the pH was adjusted in 100 mM sodium phosphate buffer to pH 7. Data analysis was carried out using the program EHTIT developed by Hellwig et al. (*20*). EHTIT yields the midpoint potentials E_m and the number n of transferred electrons by adjusting a calculated Nernst curve to the measured absorbance change at a single wavelength by an interactive fit.

Alternatively, the electrochemical titrations were performed in a thin-layer spectroelectrochemical cell of 180 μm path length mounted into a Perkin-Elmer diode array UV/vis spectrophotometer. The longer light path allowed the recording of optical spectra at a relatively low SoxXA protein concentration of 100 μM. The protein was dissolved in a 100 mM potassium phosphate buffer, pH 7.0, or in a 100 mM Tris buffer at pH 6.0 or pH 8.0. In all cases 100 mM KCl was added. In these experiments the gold grid working electrode was not modified. This enabled measurements down to −600 mV. The same mediator cocktail as described by Moss et al. (*21*) was used at a concentration of 10 μM for each mediator. To avoid an excessive exposure of the solutions to low-wavelength light from the spectrophotometer, a cutoff filter (320 nm) was employed. UV/vis spectra were recorded every 30 s while scanning a cyclic voltammogram (after an equilibration time of 100 s) with a scan rate of 0.2 mV/s and a scan increment of 20 mV. Potentials were measured vs an Ag/AgCl/1 M KCl reference electrode, which was calibrated by performing an experiment in the same cell with methyl viologen (MV) dissolved in the same buffer as a standard. For the first redox transition (MV^{2+}/MV^{+}) a reduction potential of −488 mV vs NHE was adopted. To obtain the E_m values of the heme groups in SoxXA and SoxX, the absorbance vs potential profiles of the heme α-band (552 nm) were fitted to the Nernst equation.

EPR Spectroscopy. EPR spectra were recorded at low temperatures (10 K) on a Bruker ESP300 spectrometer (S-band spectra) and a Bruker ELEXSYS E500 spectrometer (X-band spectra). The S-band spectra (2.54 GHz) were recorded using a Bruker split ring resonator inside an Oxford CF935 helium flow cryostat while for the X-band experiments (9.627 GHz) a standard TE102 cavity and an Oxford ESR910 helium flow cryostat were employed. Accurate values of the microwave frequency were obtained using a HP5352B frequency counter. Spectral simulations were performed using a home-written computer program developed by F. Neese. EPR samples for the redox titrations were obtained by sampling the reaction mixture in an electrochemical cell equilibrated at the desired potential. The protein concentration in this case was 100 μM in a 100 mM potassium phosphate buffer, pH 7.0, while the mediators were present at 10 μM each.

Analytical Procedures. The mass of SoxXA was determined by matrix-assisted laser desorption ionization (MALDI) mass spectrometry (Voyager; Perceptive Biosystems, Manchester, U.K.). Protein was determined from cell free extracts by the method of Bradford (*22*).

RESULTS

Electrochemical Titrations. The potential dependent development of the SoxXA complex from *P. pantotrophus* was monitored using two different electrochemical approaches. A thin-layer UV/vis cell (180 μm, uncoated gold electrode) was used for monitoring optical spectra (330−800 nm) while continuously scanning the potential range between +200 and −600 mV. The pH of the solution containing SoxXA and a cocktail of different redox mediators was adjusted to pH 7 using a 100 mM sodium phosphate buffer or to pH 6 and pH 8 using a 100 mM Tris buffer. The individual oxidative and reductive waves often showed a hysteresis despite the slow scan rate of 0.2 mV/s. This is due to the fact that the redox reaction for some mediators was not fully reversible in the studied potential range. The averaged normalized intensities of the oxidative and reductive waves, as monitored at 552 nm, corresponding to the heme α-band, are displayed in Figure 3A. The waves were fitted to the Nernst equation and yielded single electron transitions ($n = 0.88-0.97$). The obtained E_m values amount to +189 ± 10 mV and −432 ± 10 mV (NHE) at pH = 7.0. As can be seen from the data curves taken at different pH values, the transition at −432 mV (pH = 7) depends on pH by approximately −45 mV/pH unit, whereas the position of the transition at +189 mV remained unchanged.

Furthermore, at pH = 7.0 the potential dependent development of the SoxXA protein from *P. pantotrophus* was monitored at 417 nm (Soret band) in an ultrathin ($d = 5$ μm) electrochemical cell equipped with a modified gold electrode in the potential range 370−50 mV corresponding to the first redox transition (Figure 3B, solid circles). Using the same method, the titration of the isolated SoxX subunit was monitored (Figure 3B, empty circles). The curve for the SoxX subunit could be fitted to the Nernst equation yielding a single midpoint potential of $E_3 = 188 \pm 5$ mV (NHE) with $n = 0.9$. For the complete SoxXA protein the titration curve was extending over a somewhat broader potential range as compared to the isolated SoxX subunit. This curve could not be fitted well with one midpoint potential only. We assume that the reduction of the SoxXA protein proceeds electrochemically reversible in this setup and the solution composition follows the Nernst equation because of the small cell thickness and the coating of the working electrode. Therefore, the first reduction of the SoxXA (in which the protein is reduced by one electron as revealed by the EPR measurements, vide infra) may better be represented by the reduction of two subspecies with slightly different reduction potentials. Assuming that the two species have different extinction coefficients, the curves can be fitted with two transitions with $E_{3a} = 198$ (±5) mV and $E_{3b} = 236$ (±5) mV. The errors were estimated from the standard deviation of several titrations.

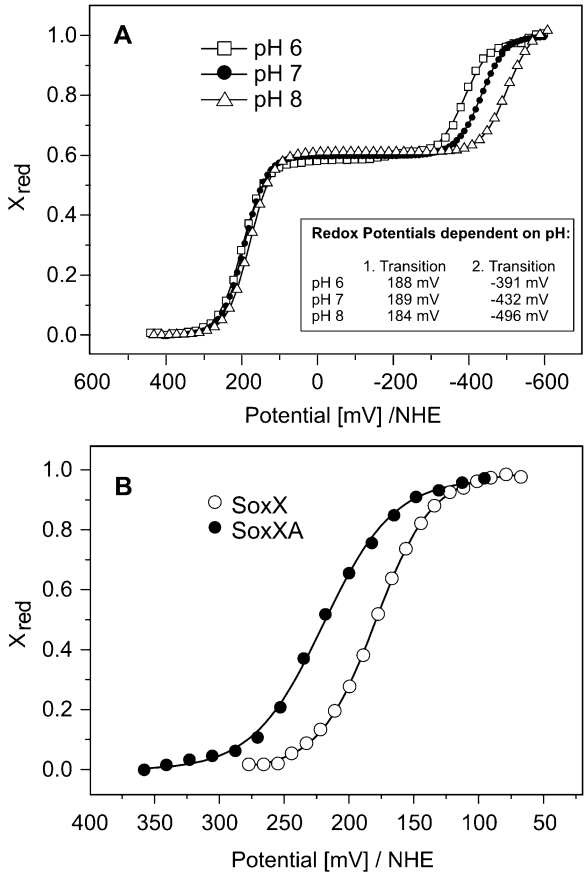

FIGURE 3: (A) UV/vis response (at 552 nm) of SoxXA in a thin wall electrochemical cell (180 μm) as a function of the electrochemical potential for pH = 6, 7, and 8. The displayed curves are averages of reductive and oxidative waves which were fitted to the Nerst curve. (B) UV/vis response (at 417 nm) of SoxXA and the isolated subunit SoxX using the ultrathin wall electrochemical cell (5 μm) with a modified gold electrode. The circles represent the measured data interactively fitted to a calculated Nernst curve. For SoxXA the theoretical Nernst fit yielded two midpoint potentials at $E_{m1} = 198 \pm 10$ mV, and $E_{m2} = 236 \pm 10$ mV (solid circles), while for SoxX (empty circles) a single midpoint potential of $E_m = 188 \pm 5$ mV was found.

EPR Spectra and Simulation. The cw-EPR spectra of SoxXA and the isolated subunit SoxX are shown in Figure 4. Spectrum A was recorded at S-band (2.54 GHz) while the spectra under (B) were measured at X-band (9.627 GHz). Since the SoxXA spectra show the same EPR spectroscopic features at both frequencies, spin−spin interaction between the individual heme centers must be smaller than the line width in these spectra which is dominated by *g*-strain. The simulation of the X-band EPR spectrum (Figure 4C, red line) therefore consists of simple additions of individually simulated heme species. The spectral analysis program EPRSIM (F. Neese, personal communication) allows the simulation and weighted addition of EPR subspectra based on their double integral, and the resulting simulation parameters are listed in Table 1. The spectrum of the separate subunit SoxX at X-band is shown in Figure 4B. The two spectra were normalized, taking into account the relative concentrations of both samples.

The EPR spectra are dominated by low-spin heme signals in the range of $g = 2.6$ to $g = 1.8$. These signals are characteristic for His/Cys coordinated heme groups (*13*, *16*, *23*). Two species (LS1 and LS2) with equal contributions

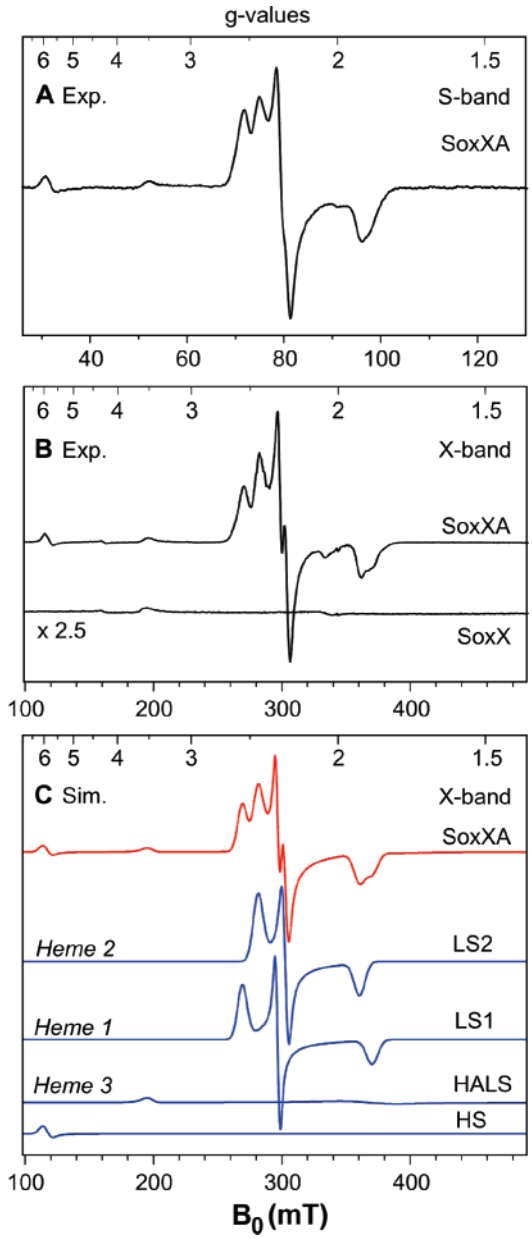

FIGURE 4: S- (A) and X-band (B) cw-EPR spectrum of SoxXA recorded at 10 K. Experimental conditions for S- and X-band: temperature 10 K, microwave power 10 μW, modulation amplitude 1 mT, modulation frequency 100 kHz, time constant and conversion time 82 ms, and recording time 15 min. (C) Decomposition of the simulated X-band EPR spectrum (indicated in red) into the species LS1 (heme 1), LS2 (heme 2), and HALS (heme 3) and the residual high-spin species (HS).

(weight = 1.0) were fitted to the EPR spectra. At $g = 3.45$ a small peak was detected, which is diagnostic for a highly anisotropic low-spin (HALS) species. Typically a His/His or His/Met ligation of the heme group is observed for HALS species. HALS species are characterized by a g_{max} signal larger than $g_z = 3.0$; the other *g*-tensor components are not easily detected (*23*−*26*). In the simulation g_x and g_y were set arbitrarily to values of 1.85 and 0.9. In most HALS model complexes these values lie in the range of $g_y = 1.8-2.1$ and $g_x = 0.5-1.0$ while obeying the relation $g_x^2 + g_y^2 + g_z^2 = 16$ (*23*). Since extreme line broadening often hinders the detection of g_y and g_x, their line width parameters were set to relatively high values. Although the intensity of the g_{max} signal is rather low, the contribution of the HALS species is

Table 1: Simulation Parameters of the EPR Spectra Shown in Figure 4 for the Individual Spectroscopically Different Heme Species in SoxXA of *P. pantotrophus*[a]

					W_z (mT) for frequency band		W_y (mT) for frequency band		W_x (mT) for frequency band	
species	g_z	g_y	g_x	weight	S	X	S	X	S	X
heme 1[b]	2.54	2.30	1.85	1.0	1.4	4.3	0.7	1.9	1.2	5.3
heme 2[c]	2.43	2.26	1.90	1.0	1.4	4.5	0.8	2.6	1.4	5
heme 3[d]	3.45	1.85	0.9	0.5	1.3	4.0	5.5	20	13.4	50
HS	2.0	5.8	5.9	0.04	2.0	8.0	1.2	4.0	1.2	4.0

[a] The same set of *g*-tensor values was used in the simulation of S- and X-band EPR spectra. The error in the *g*-values was ±0.01 unit. The line width parameters (W_z, W_y, and W_x) depend on the microwave frequency (S or X-band) and are given in mT. [b] *g*-values for SoxXA (*R. sulfidophilum*) (*13*): 2.55, 2.30, 1.87. [c] *g*-values for SoxXA (*R. sulfidophilum*) (*13*): 2.42, 2.26, 1.91. [d] *g*-values for SoxXA (*R. sulfidophilum*) (*13*): $g_{max} = 3.50$.

significant. In the simulation the HALS species has a weighing factor of 0.5. The total heme content was determined to be 2.53/mol of SoxXA (*5*). Therefore, the signals LS1 and LS2 are tentatively assigned to heme 1 and heme 2 (with a weighing factor of 1 for each heme), respectively, while the HALS species corresponds to the third *c*-type heme of SoxXA, designated heme 3 (with a weighing factor of 0.5). To clearly differentiate the signals of heme 3 of SoxX of *P. pantotrophus*, the subunit was produced in *E. coli* after heterologous expression of *SoxX* and purified to homogeneity from the periplasm. EPR spectra from the isolated SoxX subunit clearly allowed the assignment of the HALS species (heme 3) to this subunit (Figure 4B). The specific intensity of the SoxX HALS spectrum was, however, 2−3 times lower than that observed in the complete SoxXA complex. Therefore, in Figure 4B a scaling factor of 2.5 was used. The reason for the apparent lability of the HALS species is presently unknown.

The EPR spectra of the SoxXA complex also exhibit a typical high-spin heme signal at $g = 6$ (Figure 4), and this signal was not present in the spectrum of the isolated subunit SoxX (Figure 4B). From SoxXA the signal intensity of this high-spin heme (HS) contributes only with a weighting factor of 0.04 to the simulation, which corresponds to 2% of the total heme. Due to its large transition moment high-spin heme often tends to dominate EPR spectra, even if it is only a minor part of the sample (*24*−*26*). The additional EPR signals at $g = 4.3$ and around $g = 2$ might have corresponded to small Fe(III) and Cu(II) impurities in the sample. The decomposition of the simulated X-band spectrum of SoxXA into the four subspecies is presented in Figure 4C.

EPR-Monitored Electrochemical Titrations. In order to assign the observed redox transitions to the respective heme species, EPR spectra of the SoxXA complex were recorded as a function of the solution potential after chemical reduction with dithionite and titanium(III) citrate. The results for the first reduction in the potential range around +200 (±50) mV are presented in Figure 5 (lower two traces). To maintain the redox equilibrium during the sample transfer at potentials lower than −400 mV for the second reduction, a 20-fold excess of either dithionite or titanium(III) citrate was used. The EPR spectra obtained in these experiments are also shown in Figure 5 (upper two traces).

The electrochemical reduction clearly showed that the HALS species was reduced between +150 and +250 mV while the EPR spectrum of the LS2 species only fully disappeared upon 20-fold excess of titanium(III) citrate. The EPR experiments were, therefore, consistent with the optical

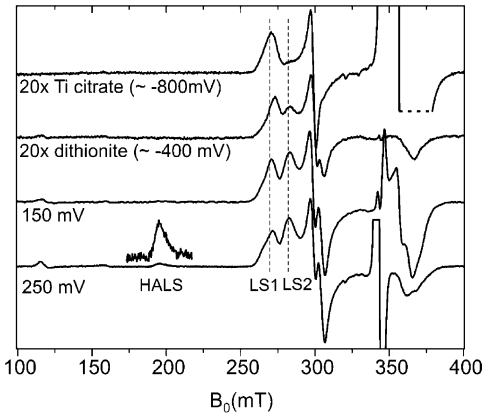

FIGURE 5: Development of SoxXA EPR spectra upon progressive chemical reduction with titanium(III) citrate and dithionite. The lower two spectra were obtained from protein solutions in phosphate buffer, pH 7, with mediators and chemically poised to the indicated potential. The upper two spectra were obtained from solutions without mediators but with excess reductant. The reduction potentials were estimated.

titrations and allowed the unequivocal assignment of the +186 mV transition to the HALS species and the −430 mV transition to LS2. The remaining heme species (LS1) was remarkably resistant to reduction: The EPR spectrum of the oxidized LS1 was still present at a potential at which all other iron species (including high-spin and inorganic impurities) were reduced.

DISCUSSION

On the basis of the X-ray crystal structure of SoxXA of *P. pantotrophus* (PDB code 2C1D) (*14*), the comparison to SoxAX from *R. sulfidophilum* (*13*, *15*), and the EPR and electrochemical studies reported here, we assign the heme groups in SoxXA as follows:

The highly anisotropic low-spin (HALS) EPR species which was observed in the isolated SoxX subunit is assigned to heme 3, which has an axial coordination by His/Met (see Figure 2). The His ligand is part of the Cys-X-Y-Cys-His *c*-type binding motif in SoxX (the residue numbers are His65, Cys61, and Cys64). Met111 from SoxX is the sixth ligand of heme 3, which matches the analysis of amino acid sequence alignments (*13*, *14*). The other two heme groups, heme 1 and heme 2, are located in the SoxA subunit. They are assigned to EPR species LS1 and LS2 of which the EPR parameters are typical for a His/thiolate coordination (*13*, *16*, *23*). Heme 2 is located in the carboxy-terminal domain of SoxA. In both SoxXA proteins of *R. sulfidophilum* (*13*,

15) and *P. pantotrophus* (*14*), this heme has a cysteine persulfide (Css251 in *P. pantotrophus*) as the axial heme iron ligand (Figure 2). Heme 1 is located in the amino-terminal domain of SoxA and has the thiolate group of Cys143 as the axial heme iron ligand. Heme 1 and heme 2 are both anchored to the structure through Cys-X-Y-Cys-His binding motifs. There are no reduction potentials reported for His/Cys or His/Css (persulfide) ligated hemes in natural systems. From studies on model hemes, however, it has been shown that, in general, the ferric state is stabilized and the reduction potential lowered when the σ donor ability of the axial ligand is increased (*27*). Based on pK_a values, the thiolate (pK_a of 8−10) should be a better σ donor to the ferric state than persulfide (*28*), thus lowering its reduction potential relative to the persulfide ligand. This logic would support the assignment of EPR species LS2 to heme 2 (which has a persulfide ligand and is reducible) and LS1 to heme 1 (which has a thiolate ligand and is not reducible).

Notably, the cw X-band EPR spectrum for SoxAX from *R. sulfidophilum* (*13*) is very similar to that of SoxXA from *P. pantotrophus* in our current study. The *g*-components of the heme 1−3 spectra of both proteins are almost identical (Table 1). The EPR line width in the spectrum of SoxAX from *R. sulfidophilum* is somewhat more narrow as compared to SoxXA from *P. pantotrophus*. This could indicate a slightly more heterogeneous binding situation for the heme groups in SoxXA from *P. pantotrophus*. On the other hand, the species LS2 in *R. sulfidophilum* occurs in a preparation-dependent mixture of two environments (*13*) whereas LS2 (heme 2) of *P. pantotrophus* occurs in a pure state. One difference between the two proteins might be that SoxXA from *P. pantotrophus* is isolated in a pure state for heme 2,which is coordinated by a persulfide cysteine. For SoxAX from *R. sulfidophilum* the dominant species in the crystal structure also contains the persulfide coordination, but in frozen solution an additional preparation-dependent LS1 EPR contribution is observed for heme 2, suggesting a "regular" cysteine coordination. Apparently, during isolation, the catalytic cycle of the two proteins gives rise to different ratios in intermediate sulfur species in the active site.

Electrochemical analysis of the SoxXA protein at pH = 7.0 revealed mid-potentials at +189 and −432 mV for the HALS and LS2 species, respectively. The HALS transition was studied additionally with an ultrathin electrochemical cell. In these experiments some broadening was observed such that the best fit to the Nernst equation was obtained using two mid-potentials, one at +198 mV and one at +236 mV. The slight broadening of the redox transition under certain conditions might be assigned to a variability of the axial ligand(s). It should be noted that the EPR HALS species is populated to only 50% in the complete SoxXA protein and less than 25% in the isolated SoxX subunit. The crystal structure indicated a substantial flexibility of the SoxX subunit especially in the interface to the SoxA subunit. It is therefore reasonable to assume that a slight variability of the methionine ligand could occur which would cause a substantial broadening of the EPR spectrum such that only a limited range of structures is observable in the EPR spectrum. But all structures might be electrochemically active, albeit with slightly different reduction potentials.

Heme 2 bound to the SoxA subunit is reduced at the very negative reduction potential of −430 mV (pH = 7.0). According to the proposed overall mechanism of the Sox system (Figure 1), SoxYZ is able to reduce SoxXA in the presence of thiosulfate (as substrate). Since the addition of thiosulfate to the sulfhydryl group of SoxY represents a two-electron oxidation, one would expect that two hemes of SoxXA will be reduced: heme 3 (HALS) and heme 2 (LS2). Both have reduction potentials below that of cytochrome c_3 (+250 mV). Therefore, cytochrome c_3 can act as an electron acceptor, and our data seem to be consistent with the proposed model of the Sox mechanism. It is not completely clear why the heme 2 potential is so negative as compared to heme 3. The results obtained on the analogous SoxAX proteins from *R. sulfidophilum* (*13*) and *Starkeya novella* (*16*) suggest that the redox potentials of heme 3 and heme 2 are almost identical. On the other hand, no EPR electrochemical titrations have been presented for these systems, and it seems that these proteins exhibit a stronger heme ligand variability than SoxXA from *P. pantotrophus*. In contrast to SoxXA from *P. pantotrophus* the protein from *S. novella* (*16*) has a strongly pH-dependent redox behavior for heme 3 while the heme 2 EPR spectrum (LS2) shows several coexisting conformations (heme 1 is lacking in this protein). The SoxAX protein from *R. sulfidophilum* (*13*) exhibits a similar variability for LS2. The SoxXA protein from *P. pantotrophus* seems remarkably stable in this respect, i.e., pH-dependent redox behavior only for LS2 and low ligand variability in general except for the HALS species. The persulfide ligand to heme 2 is known to stabilize the anionic form of the sulfhydryl of cysteine. This might lead to a rather negative redox potential. It is very likely that the observed LS2 species (persulfide-coordinated heme) represents a resting (intermediate) state formed during isolation from the thiosulfate-bound reaction intermediate. This could occur if no electron acceptor (cytochrome c_3) was available and the bound thiosulfate is reduced upon release of sulfite. SoxYZ, possibly in combination with thiosulfate as substrate, will reactivate the active site by removing one sulfur from the persulfide group. This will probably lower the reduction potential of heme 2 such that the binding of a new thiosulfate is facilitated. The pH dependence of the heme 2 mid-potential might be due to the protonation of Arg247 in the active site. This residue is proposed to provide an anionic binding pocket for the thiosulfate substrate and orient the sulfane sulfur toward the catalytic cysteine residue Cys251 (*15*).

The role of heme 1 in the C-terminal region of chain B is still an open question. The distance to heme 2 is too large (24 Å) for any electron transfer. Clearly, heme 1 cannot be directly involved in the catalytic cycle of the SoxXA enzyme. In several members of the SoxA family the Cys-Xaa-Xaa-Cys-His heme binding motif seems to be absent and is replaced by a disulfide bridge (*16*). It may be that the heme 1 site is a product of gene duplication and that the general protein fold in this region fulfills a structural role but that the heme cofactor itself is not essential for the function of the enzyme.

CONCLUSIONS

The three heme centers of SoxXA from *P. pantotrophus* have been identified and assigned unequivocally and characterized by EPR spectroscopy. Only heme 2 (SoxA C-terminal region) and heme 3 (SoxX subunit) are reducible under physiological conditions and seem to participate in

the catalytic cycle. Heme 1 (SoxA N-terminal region) is not reducible and probably not relevant for the catalytic mechanism. Since it is missing in several Sox proteins from other organisms, it is tempting to suggest that the heme binding fold only has a structural role for the protein. While the redox potential of heme 3 (HALS) is quite representative for a *c*-type cytochrome (+189 mV), the mid-potential of heme 2 (i.e., binding site of thiosulfate and the docking site of the SoxY protein) is unusually low (−432 mV). This effect is tentatively assigned to the presence of the persufide ligand which stabilizes the anionic form of the sulfhydryl group. The presence of the essential arginine residue (Arg247) in the heme 2 active site results in the pH-dependent redox behavior of heme 2.

ACKNOWLEDGMENT

We thank J. Ringk for expert technical assistance in SoxXA and SoxX purification and G. Klihm and F. Reikowski for technical support during the EPR measurements. Also, we thank an anonymous reviewer for drawing our attention to the electrochemical studies on model heme complexes which support our assignment of LS1 and LS2.

REFERENCES

1. Kelly, D. P., Shergill, J. K., Lu, W. P., and Wood, A. P. (1997) Oxidative metabolism of inorganic sulfur compounds by bacteria, *Antonie Van Leeuwenhoek 71*, 95−107.
2. Friedrich, C. G., Rother, D., Bardischewsky, F., Quentmeier, A., and Fischer, J. (2001) Oxidation of reduced inorganic sulfur compounds by bacteria: Emergence of a common mechanism?, *Appl. Environ. Microbiol. 67*, 2873−2882.
3. Friedrich, C. G., Bardischewsky, F., Rother, D., Quentmeier, A., and Fischer, J. (2005) Prokaryotic sulfur oxidation, *Curr. Opin. Microbiol. 8*, 253−259.
4. Rainey, F. A., Kelly, D. P., Stackebrandt, E., Burghardt, J., Hiraishi, A., Katayama, Y., and Wood, A. P. (1999) A re-evaluation of the taxonomy of *Paracoccus denitrificans* and a proposal for the combination *Paracoccus pantotrophus* comb. nov, *Int. J. Syst. Bacteriol. 49*, 645−651.
5. Friedrich, C. G., Quentmeier, A., Bardischewsky, F., Rother, D., Kraft, R., Kostka, S., and Prinz, H. (2000) Novel genes coding for lithotrophic sulfur oxidation of *Paracoccus pantotrophus* GB17, *J. Bacteriol. 182*, 4677−4687.
6. Rother, D., Henrich, H. J., Quentmeier, A., Bardischewsky, F., and Friedrich, C. G. (2001) Novel genes of the sox gene cluster, mutagenesis of the flavoprotein SoxF, and evidence for a general sulfur-oxidizing system in *Paracoccus pantotrophus* GB17, *J. Bacteriol. 183*, 4499−4508.
7. Quentmeier, A., and Friedrich, C. G. (2001) The cysteine residue of the SoxY protein as the active site of protein-bound sulfur oxidation of *Paracoccus pantotrophus* GB17, *FEBS Lett. 503*, 168−172.
8. Quentmeier, A., Kraft, R., Kostka, S., Klockenkamper, R., and Friedrich, C. G. (2000) Characterization of a new type of sulfite dehydrogenase from *Paracoccus pantotrophus* GB17, *Arch. Microbiol. 173*, 117−125.
9. Bardischewsky, F., Quentmeier, A., Rother, D., Hellwig, P., Kostka, S., and Friedrich, C. G. (2005) Sulfur dehydrogenase of *Paracoccus pantotrophus*: The heme-2 domain of the molybdoprotein cytochrome *c* complex is dispensable for catalytic activity, *Biochemistry 44*, 7024−7034.
10. Epel, B., Schaefer, K. O., Quentmeier, A., Friedrich, C., and Lubitz, W. (2005) Multifrequency EPR analysis of the dimanganese cluster of the putative sulfate thiohydrolase SoxB of *Paracoccus pantotrophus*, *J. Biol. Inorg. Chem. 10*, 636−642.
11. Mukhopadhyaya, P. N., Deb, C., Lahiri, C., and Roy, P. (2000) A soxA gene, encoding a diheme cytochrome *c*, and a sox locus, essential for sulfur oxidation in a new sulfur lithotrophic bacterium, *J. Bacteriol. 182*, 4278−4287.
12. Appia-Ayme, C., Little, P. J., Matsumoto, Y., Leech, A. P., and Berks, B. C. (2001) Cytochrome complex essential for photosynthetic oxidation of both thiosulfate and sulfide in *Rhodovulum sulfidophilum*, *J. Bacteriol. 183*, 6107−6118.
13. Cheesman, M. R., Little, P. J., and Berks, B. C. (2001) Novel heme ligation in a *c*-type cytochrome involved in thiosulfate oxidation: EPR and MCD of SoxAX from *Rhodovulum sulfidophilum*, *Biochemistry 40*, 10562−10569.
14. Dambe, T., Quentmeier, A., Rother, D., Friedrich, C., and Scheidig, A. J. (2005) Structure of the cytochrome complex SoxXA of *Paracoccus pantotrophus*, a heme enzyme initiating chemotrophic sulfur oxidation, *J. Struct. Biol. 152*, 229−234.
15. Bamford, V. A., Bruno, S., Rasmussen, T., Appia-Ayme, C., Cheesman, M. R., Berks, B. C., and Hemmings, A. M. (2002) Structural basis for the oxidation of thiosulfate by a sulfur cycle enzyme, *EMBO J. 21*, 5599−5610.
16. Kappler, U., Aguey-Zinsou, K. F., Hanson, G. R., Bernhardt, P. V., and Mcewan, A. G. (2004) Cytochrome *c*(551) from *Starkeya novella*—Characterization, spectroscopic properties, and phylogeny of a diheme protein of the SoxAX family, *J. Biol. Chem. 279*, 6252−6260.
17. Rother, D., and Friedrich, C. G. (2002) The cytochrome complex SoxXA of *Paracoccus pantotrophus* is produced in *Escherichia coli* and functional in the reconstituted sulfur-oxidizing enzyme system, *Biochim. Biophys. Acta 1598*, 65−73.
18. Hellwig, P., Behr, J., Ostermeier, C., Richter, O. M. H., Pfitzner, U., Odenwald, A., Ludwig, B., Michel, H., and Mantele, W. (1998) Involvement of glutamic acid 278 in the redox reaction of the cytochrome *c* oxidase from *Paracoccus denitrificans* investigated by FTIR spectroscopy, *Biochemistry 37*, 7390−7399.
19. Hellwig, P., Scheide, D., Bungert, S., Mantele, W., and Friedrich, T. (2000) FT-IR spectroscopic characterization of NADH:ubiquinone oxidoreductase (complex I) from *Escherichia coli*: Oxidation of FeS cluster N2 is coupled with the protonation of an aspartate or glutamate side chains, *Biochemistry 39*, 10884−10891.
20. Hellwig, P., Grzybek, S., Behr, J., Ludwig, B., Michel, H., and Mantele, W. (1999) Electrochemical and ultraviolet/visible/infrared spectroscopic analysis of heme *a* and *a*(3) redox reactions in the cytochrome *c* oxidase from *Paracoccus denitrificans*: Separation of heme *a* and *a*(3) contributions and assignment of vibrational modes, *Biochemistry 38*, 1685−1694.
21. Moss, D., Nabedryk, E., Breton, J., and Mantele, W. (1990) Redox-linked conformational-changes in proteins detected by a combination of infrared-spectroscopy and protein electrochemistry—Evaluation of the technique with cytochrome-*c*, *Eur. J. Biochem. 187*, 565−572.
22. Bradford, M. M. (1976) Rapid and sensitive method for quantitation of microgram quantities of protein utilizing principle of protein-dye binding, *Anal. Biochem. 72*, 248−254.
23. Walker, F. A. (1999) Magnetic spectroscopic (EPR, ESEEM, Mossbauer, MCD and NMR) studies of low-spin ferriheme centers and their corresponding heme proteins, *Coord. Chem. Rev. 186*, 471−534.
24. Fahnenschmidt, M., Rau, H. K., Bittl, R., Haehnel, W., and Lubitz, W. (1999) Characterization of a de novo designed heme protein by EPR and ENDOR spectroscopy, *Chem.—Eur. J. 5*, 2327−2334.
25. Fahnenschmidt, M., Bittl, R., Rau, H. K., Haehnel, W., and Lubitz, W. (2000) Electron paramagnetic resonance and electron nuclear double resonance spectroscopy of a heme protein maquette, *Chem. Phys. Lett. 323*, 329−339.
26. Fahnenschmidt, M., Bittl, R., Schlodder, E., Haehnel, W., and Lubitz, W. (2001) Characterization of de novo synthesized four-helix bundle proteins with metalloporphyrin cofactors, *Phys. Chem. Chem. Phys. 3*, 4082−4090.
27. Kadish, K. M., Van Caemelbecke, E., Gueletii, E., Fukuzumi, S., Miyamoto, K., Suenobu, T., Tabard, A., and Guilard, R. (1998) Kinetic and thermodynamic studies of iron(III) and iron(IV) sigma-bonded porphyrins. Formation and reactivity of [(OEP)Fe(R)](n+), where OEP is the dianion of octaethylporphyrin (n = 0, 1, 2, 3) and R = C_6H_5, 3,4,5-$C_6F_3H_2$, 2,4,6-$C_6F_3H_2$, C_6F_4H, or C_6F_5, *Inorg. Chem. 37*, 1759−1766.
28. Everett, S. A., Folkes, L. K., Wardman, P., and Asmus, K. D. (1994) Free-radical repair by a novel perthiol—Reversible hydrogen-transfer and perthiyl radical formation, *Free Radical Res. 20*, 387−400.

BI7003526